Published in final edited form as:
Biochem J. 2012 July 1; 445(1): 47–56. doi:10.1042/BJ20120408.

Distinctive Binding of Three Antagonistic Peptides to the Ephrin-Binding Pocket of the EphA4 Receptor

Ilaria Lamberto, **Haina Qin**, **Roberta Noberini**, **Lakshmanane Premkumar**, **Caroline Bourgin**, **Stefan J. Riedl**, **Jianxing Song**[*], and **Elena B. Pasquale**[*,]

[*]Sanford-Burnham Medical Research Institute, 10901 N Torrey Pines Rd, La Jolla, CA 92037, USA

[†]Department of Biological Sciences, Faculty of Science, Yong Loo Lin School of Medicine, National University of Singapore, Singapore 11926

[‡]Department of Biochemistry, Yong Loo Lin School of Medicine, National University of Singapore, Singapore 11926

[§]Department of Pathology, University of California, San Diego, CA 92093, USA

SYNOPSIS

The EphA4 receptor tyrosine kinase interacts with ephrin ligands to regulate many processes, ranging from axon guidance and nerve regeneration to cancer malignancy. Thus, antagonists that inhibit ephrin binding to EphA4 could be useful for a variety of research and therapeutic applications. Here we characterize the binding features of three antagonistic peptides (KYL, APY and VTM) that selectively target EphA4 among the Eph receptors. Isothermal titration calorimetry analysis demonstrates that all three peptides bind to the ephrin-binding domain of EphA4 with low micromolar affinity. Furthermore, the effects of a series of EphA4 mutations suggest that the peptides interact in different ways with the ephrin-binding pocket of EphA4. Chemical shifts observed by NMR spectroscopy upon binding of the KYL peptide involve many EphA4 residues, consistent with extensive interactions and possibly receptor conformational changes. Additionally, systematic replacement of each of the 12 amino acids of KYL and VTM identify the residues critical for EphA4 binding. The peptides exhibit a long half-life in cell culture medium, which with their substantial binding affinity and selectivity for EphA4 makes them excellent research tools to modulate EphA4 function.

Keywords

receptor tyrosine kinase; antagonist; targeting; imaging; nerve regeneration; cancer

INTRODUCTION

The Eph receptors are a large family of receptor tyrosine kinases with many functions in physiology and disease [1]. They bind their activating ligands, the ephrins, mainly through a

[1]To whom correspondence should be addressed: Sanford-Burnham Medical Research Institute, 10901 N. Torrey Pines Rd., La Jolla CA 92037. Phone: (858) 646-3131. Fax: (858) 646-3199. elenap@sanfordburnham.org.

AUTHOR CONTRIBUTIONS

IL generated most of the EphA4 mutants and carried out the ELISA experiments; RN generated the EphA4 Q43A mutant and carried out initial ELISA experiments; HQ performed the NMR experiments and computer modeling; LP generated EphA4 protein for the isothermal titration calorimetry experiments; CB performed the peptide pulldown experiments; JS, SJR and EBP helped with design and interpretation of the experiments and supervised the work; IL and EBP wrote the manuscript with help from the other authors.

high-affinity binding pocket located in the N-terminal ephrin-binding domain [2, 3]. A cysteine-rich region and two fibronectin type III domains connect the ephrin-binding domain to the transmembrane segment. The cytoplasmic portion of the Eph receptors includes a juxtamembrane segment, the kinase domain, a sterile-alpha-motif (SAM) domain and a C-terminal PDZ domain-binding motif. Interaction between Eph receptors and ephrin ligands, which are attached to the cell surface through a GPI-anchor (ephrin-As) or a transmembrane domain (ephrin-Bs), typically occurs at sites of cell-cell contact. Ephrin binding promotes activation of the receptor's kinase domain, triggering "forward" signals [4]. Ephrin ligands engaged with Eph receptors can also affect the cells in which they are expressed by mediating "reverse" signals.

EphA4 is highly expressed in the nervous system. The repulsive effects of EphA4 in neurons help guide the growth of developing axons towards their synaptic targets and may contribute to inhibition of axon regeneration following injury [5–12]. In addition, EphA4 is highly expressed in adult hippocampal neurons, where it controls synaptic morphology and plasticity [13–18], and experiments in mice suggest a role for EphA4 in the behavioral responses to cocaine administration [19]. Other evidence suggests that EphA4 contributes to maintain brain neural stem cells in an undifferentiated state [20]. This is in contrast to muscle, where EphA4 may contribute to myoblast differentiation [21]. Finally, increasing evidence suggests a possible role of EphA4 in several types of cancer, including glioblastoma, gastric, pancreatic, prostate and breast cancer [22–28]. EphA4 is also highly upregulated in Sezary syndrome, a leukemic variant of cutaneous T-cell lymphomas [29]. Hence, inhibiting EphA4-ephrin interaction could be useful for promoting axon regeneration and regulating synaptic plasticity in the nervous system as well as inhibiting the progression of some types of cancer.

Short peptides and small molecules that antagonize Eph receptor-ephrin interactions represent useful tools to interfere with the Eph receptor/ephrin system [30, 31]. An advantage of these artificial ligands is that they can be much more selective than the physiological ephrin ligands. Each of the five ephrin-A ligands can bind to most of the nine EphA receptors and each of the three ephrin-B ligands can bind to the five EphB receptors, whereas peptides that target only a single Eph receptor have been identified [13, 32, 33]. The EphA4 receptor is particularly promiscuous and can bind both ephrin-A and ephrin-B ligands [34–37] as well as a number of peptides and small molecules identified in various screens [13, 38–40]. Consistent with its ability to bind diverse ligands, the ephrin-binding pocket of EphA4 can assume multiple conformations [41, 42].

By screening an M13 phage display library using the entire extracellular domain of mouse EphA4 fused to the Fc portion of human IgG_1 and a C-terminal histidine tag, we previously identified four 12 amino acid-long peptides that when displayed on phage bind selectively to EphA4 and not other Eph receptors [13]. Three of the corresponding synthetic peptides – including KYL (KYLPYWPVLSSL), APY (APYCVYRGSWSC) and VTM (VTMEAINLAFPG) – also inhibit EphA4-ephrin-A5 interaction in ELISA assays. The KYL peptide, which appeared to bind best to EphA4, has since been used in organotypic cultures to implicate EphA4 in chicken neural crest cell migration and mouse hippocampal axon arborization as well as in adhesion assays to demonstrate the importance of the receptor in integrin-dependent adhesion of human T-cells [13, 43, 44]. KYL was also shown to prevent growth cone collapse in chicken retinal explants and dissociated cultures of rat cortical neurons [6, 38], promote nerve regeneration and functional recovery in a rat model of spinal cord injury [6], and inhibit the adhesion of human T-cells to endothelial cells [44]. Thus, KYL can target human, mouse, rat and chicken EphA4 and may be useful for promoting nerve regeneration after injury and modulating immune responses.

The molecular features of the interaction of KYL, APY and VTM with EphA4 have not been previously elucidated and it was not known whether the three peptides share the same EphA4 binding interface or interact with the receptor in distinctive manners. Here we report that all three peptides target the ephrin-binding pocket of EphA4 and appear to interact with partially overlapping but distinct interfaces. Interestingly, several EphA4 residues that are essential for ephrin-A5 ligand binding are not critical for interaction with the peptides, suggesting differences in the mode of binding of the peptide ligands and the ephrins.

EXPERIMENTAL

Peptides

KYL, APY and VTM >95% pure were purchased from GeneScript (Piscataway, NJ). The peptides used for alanine scanning were also purchased from Genescript with minimum purity of 85%. The identity of the peptides and peptide purity were verified by HPLC and mass spectrometry. Biotinylated peptides containing a C-terminal GSGSK linker with biotin attached to the lysine side chain were synthesized using Fmoc chemistry and purified by HPLC as previously described [13]. Peptides were dissolved in DMSO at a concentration of 10 mM and in the case of KYL and APY the concentration was verified by measuring the optical density at 280 nm. The KYL peptide used for NMR analysis was produced in bacteria. A synthetic DNA sequence encoding the peptide was ligated into the plasmid pGEX-4T1 (GE Healthcare) and the recombinant plasmid was transformed into *E. coli* BL21 (DE3). The bacteria were grown at 37 °C until OD_{600} reached 0.6, induced overnight with 0.3 mM IPTG and then harvested and lysed by sonication. The GST-fused KYL peptide was purified by affinity chromatography with glutathione-sepharose beads (GE Healthcare), released by on-gel cleavage with thrombin (yielding GS-KYL, KYL with a N-terminal glycine and serine), followed by further purification by HPLC on a RP-18 column (Vydac).

Isothermal titration calorimetry

The EphA4 ephrin-binding domain (residues 29–209) was produced as described previously [45]. Briefly, a modified pET32a vector construct encoding residues 29–209 of EphA4 (GenBank accession number NP_004429) was used for protein expression in *E. coli* Rosetta-gami B (EMD4Biosciences) cells (Novagen). EphA4 was purified by affinity chromatography using nickel-NTA resin (Qiagen) followed by thrombin cleavage and subsequent size exclusion chromatography (Superdex 200, GE Healthcare) in 20 mM Tris, pH 8.0 and 100 mM NaCl. The buffer was then exchanged to 10 mM HEPES, pH 7.6 and 100 mM NaCl using a PD10 desalting column (GE Healthcare). Both EphA4 ephrin-binding domain and the peptides were diluted to obtain a final buffer containing 5% DMSO in 10 mM Hepes, pH 7.6 and 100 mM NaCl. Isothermal titration calorimetry experiments were carried out using an ITC200 calorimeter (Microcal, Northampton, MA). Two μl aliquots of a solution containing one of the peptides KYL, VTM or APY at a concentration of 1 mM were injected into the cell containing 205 μl EphA4 ephrin-binding domain solution at a concentration of 65–95μM. Experimental data were analyzed using the Origin software package from Microcal.

Site-directed mutagenesis

The construct encoding the ephrin-binding domain of human EphA4 fused to alkaline phosphatase (AP) [36] was mutated using the QuikChange site-directed mutagenesis kit (Stratagene, La Jolla, CA) following the manufacturer's instructions. Human embryonal kidney (HEK) 293T cells were grown in Dulbecco's Modified Egle Medium (DMEM) with 10% FBS, 1 mM sodium pyruvate and pen/strep. Wild-type and mutant EphA4 AP proteins were produced after transfection of the cells with Lipofectamine 2000 (Invitrogen-Life

Technologies, Carlsbad, CA). Transfected cells were passaged and the medium was changed to Opti-MEM (GIBCO/Life Technologies) when the cells reached ~70% confluence. Culture medium containing the secreted EphA4 AP proteins was collected after 1 day and then again 1 day later and concentrated approximately 50 fold using Amicon Ultra-15 Centrifugal filters (Millipore, Billerica MA). Protein concentration was estimated based on alkaline phosphatase activity [46, 47].

ELISAs

To measure the binding of wild-type and mutant EphA4 AP to ephrin-A5 Fc, ephrin-A5 Fc (R&D Systems, Minneapolis, MN) was immobilized at 0.5 μg/ml on protein A-coated 96-well plates (Pierce-Thermo Scientific, Rockford, IL) for 1 hour at room temperature in Tris-buffered saline (TBS; 50 mM Tris-HCl, 150 mM NaCl, pH7.5) with 0.01% Tween 20. The plates were washed three times in TBS with 0.01% Tween 20 and EphA4 AP was added for 1 hour. After washing away unbound EphA4 AP, the amount of bound EphA4 AP was quantified by using *p*-nitrophenyl phosphate (Pierce-ThermoScientific) diluited in SEAP buffer (105 mM diethanolamine, 0.5 mM $MgCl_2$, pH 9.8) as the substrate and measuring optical density at 405 nm. Optical density from wells coated with Fc alone was subtracted as background.

To measure inhibition of EphA4-ephrin-A5 binding by KYL, APY or VTM peptides, different concentrations of the peptides were incubated for 3 hours together with 0.05 nM wild-type or mutant EphA4 AP in protein A-coated wells on which 1 μg/ml ephrin-A5 Fc had been previously immobilized. The only exception were the ELISAs to test the VTM peptides with alanine/serine replacements, which were carried out using 1 μg/ml EphA4 Fc immobilized on protein A-coated 96-well plates and ephrin-A5 AP [48] at 0.05 nM.

To measure the binding of wild-type or mutant EphA4 AP to the biotinylated peptides, polystyrene high capacity binding plates (Corning Life Sciences, Lowell MA) where coated with 2 μg/ml streptavidin (Pierce-Thermo Scientific) diluted in borate buffer (100mM boric acid, 100 mM sodium borate, pH 8.7) for 18 hours at room temperature. The unbound streptavidin was washed away with binding buffer (50 mM Tris-HCl, 150 mM NaCl, pH7.5 with 0.01% Tween-20 and 1 mM $CaCl_2$) and the wells were blocked with 0.5% bovine serum albumin for 1 hour at room temperature. The plates were then washed 3 times with binding buffer and 0.5 μM biotinylated KYL, 2 μM biotinylated APY or 4 μM biotinylated VTM peptide in binding buffer were immobilized on the plates by overnight incubation at 4°C. The coated wells were then washed with binding buffer before addition of EphA4 AP fusion proteins for 1 hour at room temperature. After washing away unbound EphA4 AP, 1 mg/ml *p*-nitrophenil phosphate substrate in SEAP buffer was added and absorbance at 405 nm was measured. Optical density from the wells without peptide was subtracted as background.

NMR characterization of the EphA4-KYL complex

To characterize the binding of the KYL peptide to the ephrin-binding domain of EphA4 by NMR spectroscopy, two-dimensional ^{1}H-^{15}N HSQC spectra of the ^{15}N-labeled EphA4 ephrin-binding domain were acquired at an EphA4 concentration of 100 μM in the absence or in the presence of the KYL peptide at several molar ratios (1:0.5, 1:1, 1:1.5, 1:2, 1:2.5, 1:3 EphA4:KYL). Consistent with the high KYL binding affinity measured by isothermal titration calorimetry, we found that at an EphA4:KYL ratio of 1:1 most EphA4 HSQC peaks were already converted to those corresponding to the receptor in complex with KYL, and further increases in KYL concentration did not cause additional changes. Therefore, we could not assign the HSQC peaks for the EphA4-KYL complex by following progressive peak shifts as we did in the previous characterization of the interaction of the EphA4 ephrin-

binding domain with small molecules (45). Instead, we achieved the sequential assignments for the EphA4 ephrin-binding domain in complex with KYL by analyzing triple-resonance HNCACB and CBCACONH spectra acquired using a ^{15}N-^{13}C double-labeled sample in the presence of the unlabeled KYL peptide at an EphA4:KYL ration of 1:1.5. The degree of perturbation was measured by an integrated chemical shift index calculated from the formula $[(\Delta H)^2+(\Delta N)^2/5]^{1/2}$.

Computer modeling

Molecular docking for the KYL peptide and the EphA4 ephrin-binding domain was performed by using the software HADDOCK1.3 (high ambiguity driven protein-protein docking), which can use NMR chemical-shift perturbation data and mutagenesis data to derive the docking while allowing various degrees of flexibility. The docking procedure was performed in three steps. First, randomization and rigid body energy minimization; second, semi-flexible simulated annealing; third, flexible explicit solvent refinement.

According to the Haddock definition, the solution accessible residues of the EphA4 ephrin-binding domain with larger chemical shift perturbation values (> 0.3 ppm) were set as active residues. Two additional EphA4 residues, V129 and R134, were also set as active residues based on the results of the mutagenesis experiments. EphA4 residue V129 could not be assigned by NMR even in the unbound EphA4 and the HSQC peak for R134 disappears upon formation of the EphA4-KYL complex. Furthermore, KYL residues K1, Y2, W6-L9 and L12 were also set as active residues based on the results of the alanine scan.

The PDB file for GS-KYL was generated by the program CNS from the sequence of the peptide: 1,000 structures were generated during the rigid body docking, and the best 100 structures were selected for semi-flexible simulated annealing. The best 20 structures among those were selected for further refinement in according to the explicit water model, which treats water as individual solvent molecules. Docking solutions were ranked based on the average HADDOCK score. The best model of the complex was selected for further analysis and displayed by PyMOL (www.pymol.org).

Pull-down assays with KYL

Mouse brain or a previously described B35 neuroblastoma cell clone stably transfected with chicken EphA4 [16] were homogenized in HEPES lysis buffer (50 mM HEPES, pH 7.5, 150 mM NaCl, 10% glycerol, 1% Triton X-100, 5 mM KCl, 1 mM EDTA) containing phosphatase and protease inhibitors. Three to 10 μg biotinylated peptides or a biotinylated control peptide immobilized on streptavidin beads were incubated overnight at 4°C with 4 mg brain lysate or cell lysate derived from 1/5 of a nearly confluent 10 cm plate, washed several time with HEPES lysis buffer, and boiled in sample buffer. Eluted proteins were separated by SDS-PAGE and probed by immunoblotting for EphA4.

Cell imaging with KYL bound to fluorescent quantum dots

COS cells were grown in DMEM with 10% fetal bovine serum, 1 mM sodium pyruvate and pen/strep and transfected using SuperFect Transfection Reagent (Qiagen, Valencia, CA) with a pEGFP plasmid (Clontech, Mountain View, CA) encoding the chicken EphA4 extracellular and transmembrane portions (amino acids 1–576) fused to EGFP (enhanced greeen fluorescent protein), which replaces the cytoplasmic domain, or with the pEGFP-F vector (Clontech), which encodes the membrane-targeted farnesylated EGFP. One day after transfection, the cells were plated on glass coverslips precoated with 0.1 mg/ml fibronectin and labeled a day later. To label the cells, 500 nM biotinylated KYL and 20 nM streptavidin 655 nm quantum dots (Qdots, Invitrogen-Life Technologies) were incubated together in binding buffer (PBS with 1 mM $CaCl_2$ and 2% fetal bovine serum) for 20 min on ice. The

cells were then incubated on ice with the KYL peptide bound to quantum dots for 20 min, washed with ice cold PBS, 1 mM $CaCl_2$ and fixed in 4% paraformaldehyde, 4% sucrose in PBS for 10 min at room temperature. The cells were then washed again with ice cold PBS, 1 mM $CaCl_2$ and permeabilized in PBS, 0.05% Triton X-100 for 5 min. Permeabilized cells were washed with ice cold PBS and stained with DAPI for 10 min at room temperature. Coverslips were mounted onto glass slides using Pro-long Gold (Molecular Probes-Life Technologies, Grand Island, NY) and imaged under a fluorescence microscope.

Determination of peptide stability

Peptides were incubated at 37°C in medium conditioned for 3 days by subconfluent to confluent PC3 prostate cancer cells or C2C12 myoblasts, or in mouse serum at concentrations of 100 μM for KYL, 200 μM for APY or 500 μM for VTM. Aliquots were collected at different time points and used in ELISA assays measuring inhibition of EphA4 AP-ephrin-A5 Fc binding. For these assays, ephrin-A5 Fc was immobilized at 1 μg/ml for 1 hour at room temperature in protein A-coated 96-well plates as described above. Conditioned medium or serum containing the peptides were incubated in the wells at a 1:20 dilution (corresponding to final concentrations of 5 μM for KYL, 10 μM for APY and 25 μM for VTM in the absence of proteolytic degradation) with 0.05 nM EphA4 AP for 30 minutes at 4°C. These peptide concentrations yield ~80% inhibition of EphA4 AP binding to ephrin-A5 Fc. The amount of bound AP fusion protein was quantified as described above. The optical density obtained from wells coated with Fc and incubated with EphA4 AP and medium or serum was subtracted as the background. The optical density obtained from wells incubated with conditioned medium or mouse serum not containing any peptide was used to determine the 0% inhibition level (efficacy = 0) and the optical density in the presence of peptide not incubated in medium or serum was used for normalization (efficacy = 1).

RESULTS AND DISCUSSION

The KYL, APY and VTM peptides bind to the ephrin-binding domain of EphA4 with low micromolar affinity

A previous phage display screen identified the KYL, APY and VTM peptides based on their ability to bind to the extracellular portion of EphA4 [13]. However, whether the peptides bind to the high-affinity ephrin-binding pocket of EphA4 was not conclusively demonstrated. We therefore performed isothermal titration calorimetry experiments with the ephrin-binding domain of human EphA4, which yielded K_D values of 0.85 ± 0.15 μM for KYL, 1.5 ± 0.5 μM for APY and 4.7 ± 0.1 μM for VTM (Figure 1). This confirms that all three peptides target the ephrin-binding domain of EphA4 and bind with substantial affinity. Interestingly the interaction of KYL, which has the highest binding affinity, with EphA4 appears to involve a fast component followed by a slower (~400 sec) component (Figure 1). This likely implies a slow conformational change in the receptor induced by KYL binding and would be consistent with the binding of the peptide to a particular conformation of the EphA4 ephrin-binding domain followed by re-equilibration of the different unbound receptor conformations [41, 42]. In several Eph receptors the regions that form the sides of the ephrin-binding pocket (D, E and J, Kβ strands and intervening loops) can modify their positions, accommodating different ligands [35–37, 49, 50]. This is particularly evident in EphA4, which is highly promiscuous and can bind both ephrin-A and ephrin-B ligands [35–37, 41].

Residues in the ephrin-binding pocket of EphA4 that are important for the binding of the ephrin-A5 ligand

To examine whether residues within the EphA4 pocket that binds the natural ephrin ligands are also involved in binding the peptide ligands, and to identify specific amino acids that

may play an important role in the interactions, we mutated residues in the ephrin-binding domain of EphA4 fused to alkaline phosphatase (EphA4 AP) (Table 1). First, we examined the effects of the mutations on ephrin binding. ELISA assays measuring binding of the EphA4 AP mutants to the immobilized ephrin-A5 Fc ligand revealed that the T76A, F126A, I131A and R134A mutations severely impair EphA4-ephrin-A5 interaction (Table 1 and Supplementary Figure S1; numbering of the residues is according to the construct used [45], where N29 in GenBank accession number NP_004429 is the first residue). This confirms the critical importance of the four residues in ephrin binding, which was suggested by crystal structures showing their contact with bound ephrins [35, 36]. The I31A, M32A, D33A, Q43A, D123A, M136A and A165S mutations also affect ephrin-A5 binding, which is also consistent with the previous structural studies suggesting the involvement of these residues, or the corresponding residues in other Eph receptors, in ephrin binding [35, 51]. In contrast, the remaining mutations (S30A, I39A, T41A, V129A, and G132V) do not substantially affect the interaction of EphA4 with ephrin-A5, suggesting that these residues are less critical for ephrin-A5 binding.

Residues in the ephrin-binding pocket of EphA4 are differentially involved in the binding of the KYL, APY and VTM peptide ligands

To obtain information on the effect of the mutations on peptide ligand binding, we examined the binding of the EphA4 AP mutants to the biotinylated peptides immobilized on ELISA wells (Table 1; Supplementary Figure S2). Interestingly, of the four amino acid changes that severely disrupt ephrin-A5 binding, only R134A also impairs binding of all three peptides, although the effect is weak in the case of APY. The F126A mutation substantially impairs KYL and VTM but not APY binding. The I131A mutation impairs severely VTM binding, less severely KYL binding and does not affect APY binding. Interestingly the fourth mutation, T76A, does not affect KYL binding but increases APY binding and, more dramatically, VTM binding. On the other hand the T41A mutations, which does not affect ephrin-A5 binding, strongly impairs binding of all three peptides. These results reveal substantial differences in the EphA4 residues utilized for binding ephrin-A5 and the peptides.

The T41A, Q43A and A165A mutations strongly impair the binding of all three peptides, suggesting some common features in their interactions with EphA4. Additionally, however, three mutations (S30A, I31A and I39A) similarly affect the binding of KYL and APY but not VTM and four other mutations (M32A, F126A, G132V and R134A) similarly affect the binding of KYL and VTM but not APY (Table 1). Thus, KYL shares interacting residues in EphA4 with both APY and VTM, whereas APY and VTM bind most differently from each other. A complementary assay provided additional, albeit indirect, information on the effects of the mutations on the interactions between EphA4 and the peptides. This involved ELISAs measuring the ability of the peptides to antagonize EphA4-ephrin-A5 binding, which we used to evaluate those EphA4 AP mutants that retain substantial ability to interact with ephrin-A5 (Figure 2, Supplementary Figure S3). The effects of the EphA4 mutations on peptide antagonistic activity were mostly consistent with the effects on peptide binding, with a few exceptions. For example, although the APY peptide binds to the G132V EphA4 AP mutant as well as to wild-type, it does not inhibit ephrin binding to the mutant receptor. On the other hand, the VTM peptide does not bind to the A165S EphA4 AP mutant but can nevertheless inhibit ephrin binding to the mutant receptor. These discrepancies may be explained by differential binding of the peptides to the EphA4 mutant conformation that binds the ephrin compared to the mutant conformations that predominate in the absence of ephrin [41]. In addition, the KYL and VTM peptides show impaired binding to the EphA4 M32A and D33A mutants but they inhibit ephrin-A5 binding to the mutant receptors better than to wild-type. This is likely due to the fact that the mutations also weaken ephrin

binding. Overall, these results suggest that some residues in the EphA4 ephrin-binding pocket are important for the binding of all three peptides while others are critical for the binding of only one or two of the peptides. Furthermore, the three peptide ligands do not closely mimic the binding of the ephrin-A5 ligand.

To obtain a more complete overview of the residues in the EphA4 ephrin-binding domain that are involved in KYL binding, we compared the NMR heteronuclear single quantum coherence (HSQC) spectra of EphA4 alone or in complex with GS-KYL, a modified version of KYL containing an N-terminal glycine and serine derived from the bacterial expression construct. The chemical shift differences (CSD) identify a number of EphA4 residues that are affected by KYL binding (Figure 3 and Table 1), which may be caused by a direct interaction or conformational/dynamic changes occurring as a result of peptide binding [36, 41]. All the residues with high CSD values (>0.4) are located within or near the ephrin-binding pocket of EphA4 [35, 51]. They include the I31, M32, D33, T41, Q43, F126, I131, G132 and A165 residues shown to be important for KYL binding in our mutagenesis experiments. Interestingly, although the chemical shift differences for S30 and T76 are very large (Figure 3B) and the two residues have close contacts with the KYL peptide in a model of the complex (Figure 5B), mutation of these residues to alanine does not affect KYL binding (Supplementary Figure S2). This implies that the introduced alanine may not be sufficiently different from serine or threonine to substantially affect KYL binding or that the energetic contribution of the two residues to the binding of the peptide may be minor, given that the magnitude of the CSD and the contribution of a residue to the binding energy are not always correlated [52].

Residues of KYL and VTM that are critical for interaction with EphA4

To identify the residues of the KYL and VTM peptides that are important for binding to EphA4, we replaced each of their amino acids with alanine, except for the two alanines in VTM that were replaced with serine. We did not perform a similar analysis for APY, in which the two cysteines likely form a disulfide bond that cyclizes the peptide and is critical for its binding activity. Seven of the 12 amino acids in KYL (K1, Y2, W6, P7, V8, L9 and L12) and 8 of the 12 amino acids in VTM (T2, M3, E4, I6, N7, L8, F10 and P11) are essential for high affinity binding because substitution of each of these amino acids with alanine severely impairs the ability of the peptides to inhibit EphA4-ephrinA5 interaction in ELISA assays (Figure 4). The other residues play a lesser role or do not appear to play a role in EphA4 binding. For example, replacement of L3, P4, and Y5 with alanine decreases the inhibitory activity of KYL in ELISAs by only 2–4 fold, while replacement of S10 and S11 results in an IC_{50} value that is comparable to that of unmodified KYL. Furthermore, replacement of of V1, A5 and A9 reduces the inhibitory potency of VTM by only 2–4 fold, and replacement of G12 by less than 2 fold (Figure 4).

Model of the EphA4-KYL complex

We have attempted to determine the three-dimensional structure of the EphA4-KYL complex by both crystallography and NMR spectroscopy. However, attempts to co-crystallize the EphA4 ephrin-binding domain in complex with the synthetic KYL peptide led to several crystals of EphA4 without KYL. On the other hand, NMR structure determination was hindered by the extensive disappearance of NMR resonance signals for EphA4 side chains in the presence of the recombinant GS-KYL peptide. Therefore, we used the PDB 3CKH EphA4 structure for molecular docking of the GS-KYL peptide with the HADDOCK software using the information obtained from the NMR chemical shifts, EphA4 mutagenesis and alanine scanning outlined above. In the model, the KYL peptide is buried in the EphA4 ephrin-binding pocket (Figure 5A). The EphA4 residues with significant NMR perturbations and critical for binding as revealed by mutagenesis are all located in the pocket

accommodating the KYL peptide (Figure 5B). The KYL peptide is characterized by a positively charged N terminus and a rather hydrophobic middle region. In the model of the complex, side chain amide protons of KYL residue K1 form two hydrogen bonds with EphA4 E27, one with the backbone and another with side chain oxygen atoms. The aromatic ring of KYL Y2 is in close contact with EphA4 L83, a residue that undergoes a large shift upon KYL binding (Figure 3B). Hydrophobic KYL residues W6, P7, V8 and L9 establish extensive contacts with the hydrophobic patches of the ephrin-binding pocket of EphA4 (Figure 5A). For example, W6 is involved in hydrophobic contacts with EphA4 residues F126, V129, I131 and A165, in agreement with the mutagenesis and NMR titration results. Additionally, the backbone amide proton of W6 forms a hydrogen bond with the side chain oxygen of EphA4 T76, consistent with the NMR titration data indicating that T76 is significantly perturbed. However, the EphA4 T76A mutation does not substantially affect KYL binding affinity (Table 1), suggesting that T76 may make a very minor energetic contribution to KYL binding. This would not be surprising because a portion of interfacial residues in protein complexes can have a minor, or even negative, energetic contribution to the formation of complexes [52]. P7 appears to be particularly important for KYL binding because in addition to making direct contacts with EphA4 S30 and T41, it may induce and stabilize a bend in the backbone of the peptide that allows residues V8 and L9 to form hydrophobic contacts with EphA4 residues T41 and I131, respectively. This is consistent with the complete loss of binding of the P7A modified KYL (Fig. 4A–C). L12 is also essential for binding because its hydrophobic side chain bends to form a hydrophobic cluster with the side chains of P7 and L9 from KYL thus stabilizing their orientation, which is required for interaction with EphA4 residues. Moreover, the amide proton of L12 forms a hydrogen bond with the backbone oxygen of G132.

Use of EphA4-binding peptides for receptor purification and cell imaging

Given their substantial binding affinity, antagonistic properties and selectivity for EphA4 [13], the three peptides represent useful tools for a number of applications. While KYL has already been used to modulate EphA4 function in various biological systems [6, 13, 38, 43, 44], we also found that binding of all three peptides to EphA4 is sufficiently stable to enable pull-down of the receptor from cell and tissue lysates (Figure 6A,B). Thus, these peptides may be useful to purify EphA4 protein or isolate tumor cells expressing high levels of EphA4 [53–55]. Furthermore, KYL coupled to fluorescent quantum dots can be used to image cells expressing EphA4 (Figure 6C). Thus, KYL coupled to fluorescent or radioactive tags may serve to image EphA4-expressing tumors *in vivo*, similar to other Eph receptor-targeting peptides [56, 57].

Stability of KYL, APY and VTM in cell culture medium and mouse serum

To evaluate the stability of the peptides for use in cell culture experiments, we measured their ability to inhibit EphA4-ephrin-A5 interaction in ELISA assays after different incubation times in culture medium conditioned by human PC3 prostate cancer cells or mouse C2C12 myoblasts cells. The KYL and APY peptides appear to be quite stable in cell culture medium, with a half-life of ~8–12 hours in medium conditioned by PC3 and C2C12 cells (Figure 7). The VTM peptide is even more stable, with a half-life of ~30 and 90 hours, respectively. On the other hand, the antagonistic activity of the peptides is lost within 10–40 minutes of incubation in mouse serum, with VTM again being more stable than KYL and APY (Figure 7). Thus, modifications that increase the half-life of the peptides in the blood circulation will be useful for *in vivo* applications, similar to what we have observed for a peptide that targets the EphB4 receptor [58].

In conclusion, we have characterized three peptides that selectively bind to the EphA4 receptor and identified features that are important for peptide-receptor interaction. We have

generated a series of mutations in the EphA4 ephrin-binding pocket and found that many of them differentially affect the binding of the three peptide ligands as well as the natural ephrin-A5 ligand to EphA4, suggesting that each ligand interacts in a distinctive manner with residues of the high affinity ephrin-binding pocket of EphA4, perhaps by binding to different conformations of the receptor [41]. The peptides target the the high-affinity ephrin-binding pocket of EphA4, which is used by the G–H loop of all the ephrins in a promiscuous manner. In contrast, the peptides are highly selective for EphA4 [13] and therefore likely exploit unique feature of the receptor's pocket. Furthermore, the alanine scans of the KYL and VTM peptides identify amino acids that are essential for the inhibitory properties of the peptides. They also reveal that five amino acids in KYL and four in VTM do not substantially contribute to the antagonistic ability of the peptides and could therefore be modified to obtain a more powerful inhibitor or increase peptide stability. The first and the last amino acids of VTM, but not KYL, appear to be dispensable for high-affinity binding and therefore the VTM peptide may be shortened to 10 amino acids without appreciable loss of binding affinity. In future applications, KYL, APY and VTM as well as optimized derivatives could be conjugated with drugs, toxins and imaging agents or incorporated into nanoparticles to selectively target cells with high EphA4 levels.

Supplementary Material

Refer to Web version on PubMed Central for supplementary material.

Acknowledgments

The authors thank A. Bobkov for performing the isothermal titration calorimetry experiments, G. Scicolone for the EphA4-EGFP construct, and L.D. Nguyen for staining cells with KYL peptide bound to quantum dots.

FUNDING

This work was supported by NIH grants CA138390 (EBP and SR) and NS067502 (EBP), and Singapore National Medical Research Council Grant NMRC/1216/2009 (JS).

Abbreviations used

AP	alkaline phosphatase
CSD	chemical shifts difference
EGFP	enhanced greeen fluorescent protein
EGFP-F	farnesylated enhanced greeen fluorescent protein
ELISA	enzyme-linked immunosorbent assay
Fmoc	*N*-(9-fluorenyl)methoxycarbonyl
GPI	glycosylphosphatidylinositol
HSQC	heteronuclear single quantum coherence
HRP	horseradish peroxidase
NMR	nuclear magnetic resonance
pNPP	*p*-nitrophenyl phosphate
SAM	sterile alpha motif
PDZ	postsynaptic density protein, Drosophila disc large tumor suppressor, zonula occludens-1 protein

REFERENCES

1. Pasquale EB. Eph-ephrin bidirectional signaling in physiology and disease. Cell. 2008; 133:38–52. [PubMed: 18394988]
2. Seiradake E, Harlos K, Sutton G, Aricescu AR, Jones EY. An extracellular steric seeding mechanism for Eph-ephrin signaling platform assembly. Nat. Struct. Mol. Biol. 2010; 17:398–402. [PubMed: 20228801]
3. Himanen JP, Yermekbayeva L, Janes PW, Walker JR, Xu K, Atapattu L, Rajashankar KR, Mensinga A, Lackmann M, Nikolov DB, Dhe-Paganon S. Architecture of Eph receptor clusters. Proc Natl Acad Sci U S A. 2010; 107:10860–10865. [PubMed: 20505120]
4. Pasquale EB. Eph receptor signalling casts a wide net on cell behaviour. Nat. Rev. Mol. Biol. 2005; 6:462–475.
5. Connor RJ, Menzel P, Pasquale EB. Expression and tyrosine phosphorylation of Eph receptors suggest multiple mechanisms in patterning of the visual system. Dev. Biol. 1998; 193:21–35. [PubMed: 9466885]
6. Fabes J, Anderson P, Brennan C, Bolsover S. Regeneration-enhancing effects of EphA4 blocking peptide following corticospinal tract injury in adult rat spinal cord. Eur. J. Neurosci. 2007; 26:2496–2505. [PubMed: 17970742]
7. Fabes J, Anderson P, Yanez-Munoz RJ, Thrasher A, Brennan C, Bolsover S. Accumulation of the inhibitory receptor EphA4 may prevent regeneration of corticospinal tract axons following lesion. Eur. J. Neurosci. 2006; 23:1721–1730. [PubMed: 16623828]
8. Goldshmit Y, Galea MP, Wise G, Bartlett PF, Turnley AM. Axonal regeneration and lack of astrocytic gliosis in EphA4-deficient mice. J. Neurosci. 2004; 24:10064–10073. [PubMed: 15537875]
9. Kramer ER, Knott L, Su F, Dessaud E, Krull CE, Helmbacher F, Klein R. Cooperation between GDNF/Ret and ephrinA/EphA4 signals for motor-axon pathway selection in the limb. Neuron. 2006; 50:35–47. [PubMed: 16600854]
10. Kullander K, Butt SJ, Lebret JM, Lundfald L, Restrepo CE, Rydstrom A, Klein R, Kiehn O. Role of EphA4 and EphrinB3 in local neuronal circuits that control walking. Science. 2003; 299:1889–1892. [PubMed: 12649481]
11. Kullander K, Mather NK, Diella F, Dottori M, Boyd AW, Klein R. Kinase-dependent and kinase-independent functions of EphA4 receptors in major axon tract formation in vivo. Neuron. 2001; 29:73–84. [PubMed: 11182082]
12. Goldshmit Y, Bourne J. Upregulation of EphA4 on astrocytes potentially mediates astrocytic gliosis after cortical lesion in the marmoset monkey. J. Neurotrauma. 2010; 27:1321–1332. [PubMed: 20486805]
13. Murai KK, Nguyen LN, Koolpe M, McLennan R, Krull CE, Pasquale EB. Targeting the EphA4 receptor in the nervous system with biologically active peptides. Mol. Cell. Neurosci. 2003; 24:1000–1011. [PubMed: 14697664]
14. Grunwald IC, Korte M, Adelmann G, Plueck A, Kullander K, Adams RH, Frotscher M, Bonhoeffer T, Klein R. Hippocampal plasticity requires postsynaptic ephrinBs. Nat. Neurosci. 2004; 7:33–40. [PubMed: 14699416]
15. Fu WY, Chen Y, Sahin M, Zhao XS, Shi L, Bikoff JB, Lai KO, Yung WH, Fu AK, Greenberg ME, Ip NY. Cdk5 regulates EphA4-mediated dendritic spine retraction through an ephexin1-dependent mechanism. Nat Neurosci. 2007; 10:67–76. [PubMed: 17143272]
16. Bourgin C, Murai KK, Richter M, Pasquale EB. The EphA4 receptor regulates dendritic spine remodeling by affecting beta1-integrin signaling pathways. J. Cell Biol. 2007; 178:1295–1307. [PubMed: 17875741]
17. Carmona MA, Murai KK, Wang L, Roberts AJ, Pasquale EB. Glial ephrin-A3 regulates hippocampal dendritic spine morphology and glutamate transport. Proc. Natl. Acad. Sci. U. S. A. 2009; 106:12524–12529. [PubMed: 19592509]
18. Filosa A, Paixao S, Honsek SD, Carmona MA, Becker L, Feddersen B, Gaitanos L, Rudhard Y, Schoepfer R, Klopstock T, Kullander K, Rose CR, Pasquale EB, Klein R. Neuron-glia

communication via EphA4/ephrin-A3 modulates LTP through glial glutamate transport. Nat. Neurosci. 2009; 12:1285–1292. [PubMed: 19734893]

19. Kimura K, Hikida T, Yawata S, Yamaguchi T, Nakanishi S. Pathway-specific engagement of ephrinA5-EphA4/EphA5 system of the substantia nigra pars reticulata in cocaine-induced responses. Proc. Natl. Acad. Sci. U. S. A. 2011; 108:9981–9986. [PubMed: 21628570]
20. Khodosevich K, Watanabe Y, Monyer H. EphA4 preserves postnatal and adult neural stem cells in an undifferentiated state in vivo. J. Cell Sci. 2011; 124:1268–1279. [PubMed: 21444754]
21. Minami M, Koyama T, Wakayama Y, Fukuhara S, Mochizuki N. EphrinA/EphA signal facilitates insulin-like growth factor-I-induced myogenic differentiation through suppression of the Ras/extracellular signal-regulated kinase 1/2 cascade in myoblast cell lines. Mol. Biol. Cell. 2011; 22:3508–3519. [PubMed: 21795402]
22. Ashida S, Nakagawa H, Katagiri T, Furihata M, Iiizumi M, Anazawa Y, Tsunoda T, Takata R, Kasahara K, Miki T, Fujioka T, Shuin T, Nakamura Y. Molecular features of the transition from prostatic intraepithelial neoplasia (PIN) to prostate cancer: genome-wide gene-expression profiles of prostate cancers and PINs. Cancer Res. 2004; 64:5963–5972. [PubMed: 15342375]
23. Iiizumi M, Hosokawa M, Takehara A, Chung S, Nakamura T, Katagiri T, Eguchi H, Ohigashi H, Ishikawa O, Nakamura Y, Nakagawa H. EphA4 receptor, overexpressed in pancreatic ductal adenocarcinoma, promotes cancer cell growth. Cancer Sci. 2006; 97:1211–1216. [PubMed: 16965393]
24. Fukai J, Yokote H, Yamanaka R, Arao T, Nishio K, Itakura T. EphA4 promotes cell proliferation and migration through a novel EphA4-FGFR1 signaling pathway in the human glioma U251 cell line. Mol. Cancer Ther. 2008; 7:2768–2778. [PubMed: 18790757]
25. Oki M, Yamamoto H, Taniguchi H, Adachi Y, Imai K, Shinomura Y. Overexpression of the receptor tyrosine kinase EphA4 in human gastric cancers. World J. Gastroenterol. 2008; 14:5650–5656. [PubMed: 18837080]
26. Gong J, Morishita A, Kurokohchi K, Tani J, Kato K, Miyoshi H, Inoue H, Kobayashi M, Liu S, Murota M, Muramatsu A, Izuishi K, Suzuki Y, Yoshida H, Uchida N, Deguchi K, Iwama H, Ishimaru I, Masaki T. Use of protein array to investigate receptor tyrosine kinases activated in gastric cancer. Int. J. Oncol. 2010; 36:101–106. [PubMed: 19956838]
27. Tyner JW, Deininger MW, Loriaux MM, Chang BH, Gotlib JR, Willis SG, Erickson H, Kovacsovics T, O'Hare T, Heinrich MC, Druker BJ. RNAi screen for rapid therapeutic target identification in leukemia patients. Proc. Natl. Acad. Sci. U. S. A. 2009; 106:8695–8700. [PubMed: 19433805]
28. Brantley-Sieders DM, Jiang A, Sarma K, Badu-Nkansah A, Walter DL, Shyr Y, Chen J. Eph/ephrin profiling in human breast cancer reveals significant associations between expression level and clinical outcome. PLoS One. 2011; 6:e24426. [PubMed: 21935409]
29. van Doorn R, Dijkman R, Vermeer MH, Out-Luiting JJ, van der Raaij-Helmer EM, Willemze R, Tensen CP. Aberrant expression of the tyrosine kinase receptor EphA4 and the transcription factor twist in Sezary syndrome identified by gene expression analysis. Cancer Res. 2004; 64:5578–5586. [PubMed: 15313894]
30. Pasquale EB. Eph receptors and ephrins in cancer: bidirectional signalling and beyond. Nat. Rev. Cancer. 2010; 10:165–180. [PubMed: 20179713]
31. Noberini R, Lamberto I, Pasquale EB. Targeting Eph receptors with peptides and small molecules: Progress and challenges. Semin. Cell Dev. Biol. 2012; 23:51–57. [PubMed: 22044885]
32. Koolpe M, Burgess R, Dail M, Pasquale EB. EphB receptor-binding peptides identified by phage display enable design of an antagonist with ephrin-like affinity. J. Biol. Chem. 2005; 280:17301–17311. [PubMed: 15722342]
33. Koolpe M, Dail M, Pasquale EB. An ephrin mimetic peptide that selectively targets the EphA2 receptor. J. Biol. Chem. 2002; 277:46974–46979. [PubMed: 12351647]
34. Pasquale EB. Eph-ephrin promiscuity is now crystal clear. Nat. Neurosci. 2004; 7:417–418. [PubMed: 15114347]
35. Bowden TA, Aricescu AR, Nettleship JE, Siebold C, Rahman-Huq N, Owens RJ, Stuart DI, Jones EY. Structural plasticity of eph receptor A4 facilitates cross-class ephrin signaling. Structure. 2009; 17:1386–1397. [PubMed: 19836338]

36. Qin H, Noberini R, Huan X, Shi J, Pasquale EB, Song J. Structural characterization of the EphA4-Ephrin-B2 complex reveals new features enabling Eph-ephrin binding promiscuity. J. Biol. Chem. 2010; 285:644–654. [PubMed: 19875447]
37. Singla N, Goldgur Y, Xu K, Paavilainen S, Nikolov DB, Himanen JP. Crystal structure of the ligand-binding domain of the promiscuous EphA4 receptor reveals two distinct conformations. Biochem. Biophys. Res. Commun. 2010; 399:555–559. [PubMed: 20678482]
38. Noberini R, Koolpe M, Peddibhotla S, Dahl R, Su Y, Cosford ND, Roth GP, Pasquale EB. Small Molecules Can Selectively Inhibit Ephrin Binding to the EphA4 and EphA2 Receptors. J. Biol. Chem. 2008; 283:29461–29472. [PubMed: 18728010]
39. Noberini R, De SK, Zhang Z, Wu B, Raveendra-Panickar D, Chen V, Vazquez J, Qin H, Song J, Cosford ND, Pellecchia M, Pasquale EB. A disalicylic acid-furanyl derivative inhibits ephrin binding to a subset of Eph receptors. Chem. Biol. Drug Des. 2011; 78:667–678. [PubMed: 21791013]
40. Giorgio C, Hassan Mohamed I, Flammini L, Barocelli E, Incerti M, Lodola A, Tognolini M. Lithocholic Acid Is an Eph-ephrin Ligand Interfering with Eph-kinase Activation. PLoS One. 2011; 6:e18128. [PubMed: 21479221]
41. Qin H, Lim L, Song J. Protein dynamics at Eph receptor-ligand interfaces as revealed by crystallography, NMR and MD simulations. BMC Biophys. 2012; 5:2. [PubMed: 22277260]
42. Nussinov R, Ma B. Protein dynamics and conformational selection in bidirectional signal transduction. BMC Biol. 2012; 10:2. [PubMed: 22277130]
43. Galimberti I, Bednarek E, Donato F, Caroni P. EphA4 signaling in juveniles establishes topographic specificity of structural plasticity in the hippocampus. Neuron. 2010; 65:627–642. [PubMed: 20223199]
44. Sharfe N, Nikolic M, Cimpeon L, Van De Kratts A, Freywald A, Roifman CM. EphA and ephrin-A proteins regulate integrin-mediated T lymphocyte interactions. Mol. Immunol. 2008; 45:1208–1220. [PubMed: 17980912]
45. Qin H, Shi J, Noberini R, Pasquale EB, Song J. Crystal Structure and NMR Binding Reveal That Two Small Molecule Antagonists Target the High Affinity Ephrin-binding Channel of the EphA4 Receptor. J. Biol. Chem. 2008; 283:29473–29484. [PubMed: 18708347]
46. Flanagan JG, Cheng HJ, Feldheim DA, Hattori M, Lu Q, Vanderhaeghen P. Alkaline phosphatase fusions of ligands or receptors as in situ probes for staining of cells, tissues, and embryos. Methods Enzymol. 2000; 327:19–35. [PubMed: 11044971]
47. Cullen BR. Utility of the secreted placental alkaline phosphatase reporter enzyme. Methods Enzymol. 2000; 326:159–164. [PubMed: 11036641]
48. Menzel P, Valencia F, Godement P, Dodelet VC, Pasquale EB. Ephrin-A6, a new ligand for EphA receptors in the developing visual system. Dev. Biol. 2001; 230:74–88. [PubMed: 11161563]
49. Chrencik JE, Brooun A, Kraus ML, Recht MI, Kolatkar AR, Han GW, Seifert JM, Widmer H, Auer M, Kuhn P. Structural and biophysical characterization of the EphB4-ephrinB2 protein-protein interaction and receptor specificity. J. Biol. Chem. 2006; 281:28185–28192. [PubMed: 16867992]
50. Chrencik JE, Brooun A, Recht MI, Nicola G, Davis LK, Abagyan R, Widmer H, Pasquale EB, Kuhn P. Three-dimensional Structure of the EphB2 Receptor in Complex with an Antagonistic Peptide Reveals a Novel Mode of Inhibition. J. Biol. Chem. 2007; 282:36505–36513. [PubMed: 17897949]
51. Himanen JP, Rajashankar KR, Lackmann M, Cowan CA, Henkemeyer M, Nikolov DB. Crystal structure of an Eph receptor-ephrin complex. Nature. 2001; 414:933–938. [PubMed: 11780069]
52. Dauplais M, Lecoq A, Song J, Cotton J, Jamin N, Gilquin B, Roumestand C, Vita C, de Medeiros CL, Rowan EG, Harvey AL, Menez A. On the convergent evolution of animal toxins. Conservation of a diad of functional residues in potassium channel-blocking toxins with unrelated structures. J. Biol. Chem. 1997; 272:4302–4309. [PubMed: 9020148]
53. Scarberry KE, Dickerson EB, McDonald JF, Zhang ZJ. Magnetic nanoparticle-peptide conjugates for in vitro and in vivo targeting and extraction of cancer cells. J. Am. Chem. Soc. 2008; 130:10258–10262. [PubMed: 18611005]

54. Scarberry KE, Dickerson EB, Zhang ZJ, Benigno BB, McDonald JF. Selective removal of ovarian cancer cells from human ascites fluid using magnetic nanoparticles. Nanomedicine. 2010; 6:399–408. [PubMed: 19969103]

55. Scarberry KE, Mezencev R, McDonald JF. Targeted removal of migratory tumor cells by functionalized magnetic nanoparticles impedes metastasis and tumor progression. Nanomedicine. 2011; 6:69–78. [PubMed: 21182419]

56. Xiong C, Huang M, Zhang R, Song S, Lu W, Flores L 2nd, Gelovani J, Li C. In vivo small-animal PET/CT of EphB4 receptors using 64Cu-labeled peptide. J. Nucl. Med. 2011; 52:241–248. [PubMed: 21233177]

57. Zhang R, Xiong C, Huang M, Zhou M, Huang Q, Wen X, Liang D, Li C. Peptide-conjugated polymeric micellar nanoparticles for Dual SPECT and optical imaging of EphB4 receptors in prostate cancer xenografts. Biomaterials. 2011; 32:5872–5879. [PubMed: 21612822]

58. Noberini R, Mitra S, Salvucci O, Valencia F, Duggineni S, Prigozhina N, Wei K, Tosato G, Huang Z, Pasquale EB. PEGylation potentiates the effectiveness of an antagonistic peptide that targets the EphB4 receptor with nanomolar affinity. PLoS One. 2011; 6:e28611. [PubMed: 22194865]

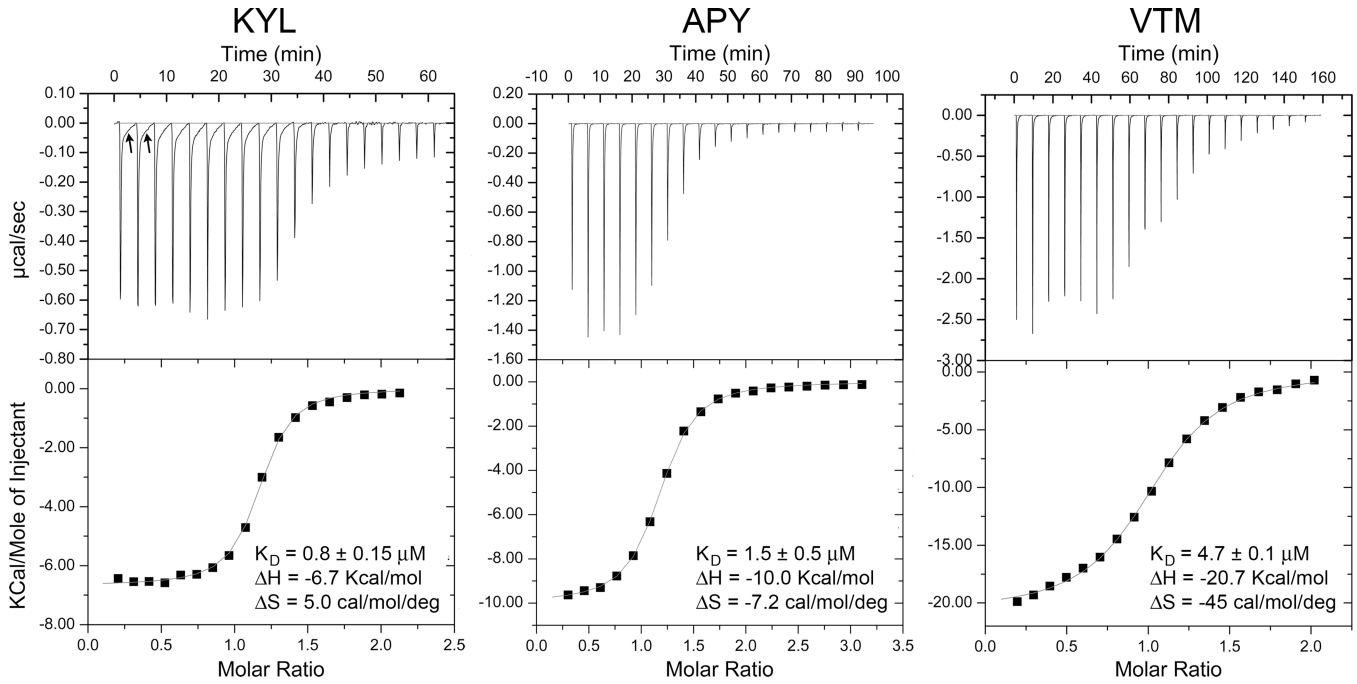

Figure 1. The KYL, APY and VTM peptides bind to the ephrin-binding domain of EphA4 with low micromolar affinity

Isothermal titration calorimetry profiles for the binding of the three peptides to EphA4 and plots of the integrated values for the reaction heats (after blank subtraction and normalization to the amount of peptide injected) versus EphA4/peptide molar ratio (lower part of each panel). Arrows in the top left panel indicate the slow component for the binding of the KYL peptide.

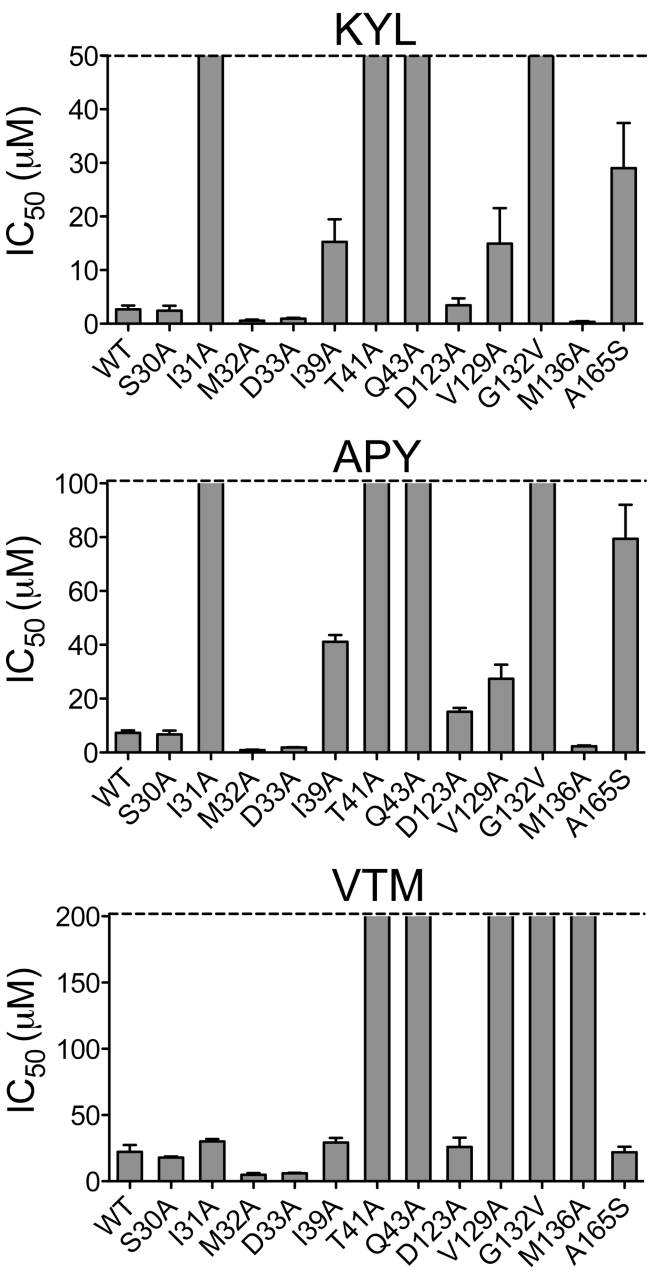

EphA4	IC_{50} ± SE (μM)
WT	2.7 ± 0.70
S30A	2.4 ± 0.89
I31A	>>100
M32A	0.5 ± 0.20
D33A	0.9 ± 0.15
I39A	15 ± 4.21
T41A	>>100
Q43A	71 ± 22
D123A	3.41 ± 1.29
V129A	15 ± 6.7
G132V	>>100
M136A	0.36 ± 0.11
A165S	29 ± 8.4
WT	7.3 ± 0.9
S30A	6.7 ± 1.3
I31A	>>100
M32A	0.89 ± 0.16
D33A	1.9 ± 0.11
I39A	41 ± 2.5
T41A	>>100
Q43A	>100
D123A	15 ± 1.5
V129A	27 ± 5.2
G132V	>100
M136A	2.3 ± 0.37
A165S	79 ± 13
WT	22 ± 5.1
S30A	18 ± 0.7
I31A	30 ± 1.8
M32A	4.9 ± 1.3
D33A	6.0 ± 0.41
I39A	29 ± 3.4
T41A	>>100
Q43A	>>100
D123A	26 ± 6.9
V129A	>>100
G132V	>>100
M136A	>>100
A165S	21 ± 4.2

Figure 2. EphA4 mutagenesis identifies residues important for KYL, APY and VTM binding

The histograms show averages IC_{50} values ± SE for the inhibition of wild-type and the indicated EphA4 AP mutants to immobilized ephrin-A5 Fc. The averages for each peptide ± SEM, each calculated from the indicated number of inhibition curves (n), are listed in the table at the right of each histogram.

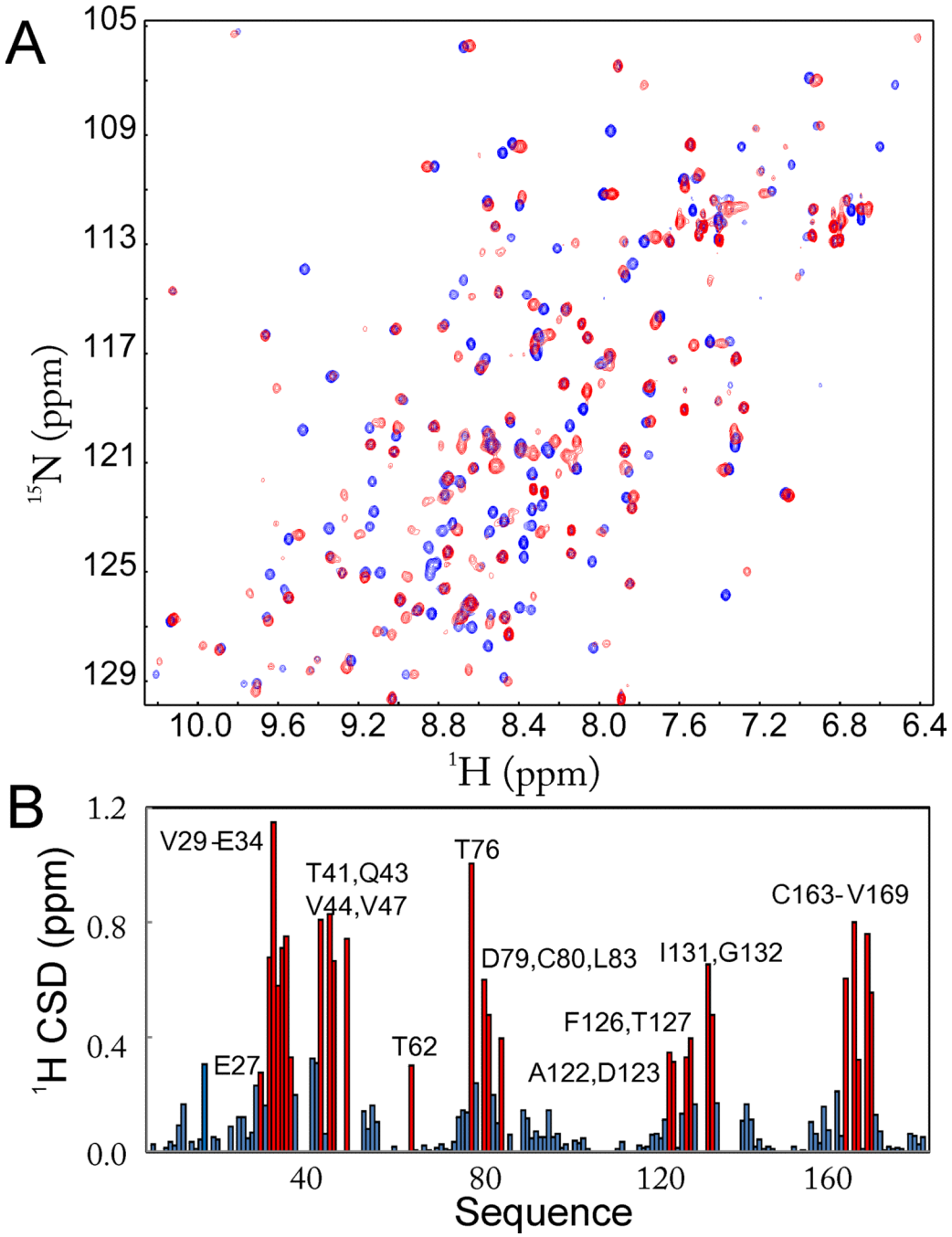

Figure 3. Chemical shifts identify residues in the EphA4 ephrin-binding domain that are affected by KYL binding

(**A**) ^{1}H-^{15}N NMR spectra of the EphA4 ephrin-binding domain in the absence (blue) and in the presence (red) of KYL peptide at a ratio of 1:1. (**B**) Histogram showing residue-specific chemical shift differences (CSDs) for the EphA4 ephrin-binding domain induced by KYL binding. The molar ration of EphA4 to KYL in these experiments was 1:1.5. Residues used for molecular docking are labeled in red.

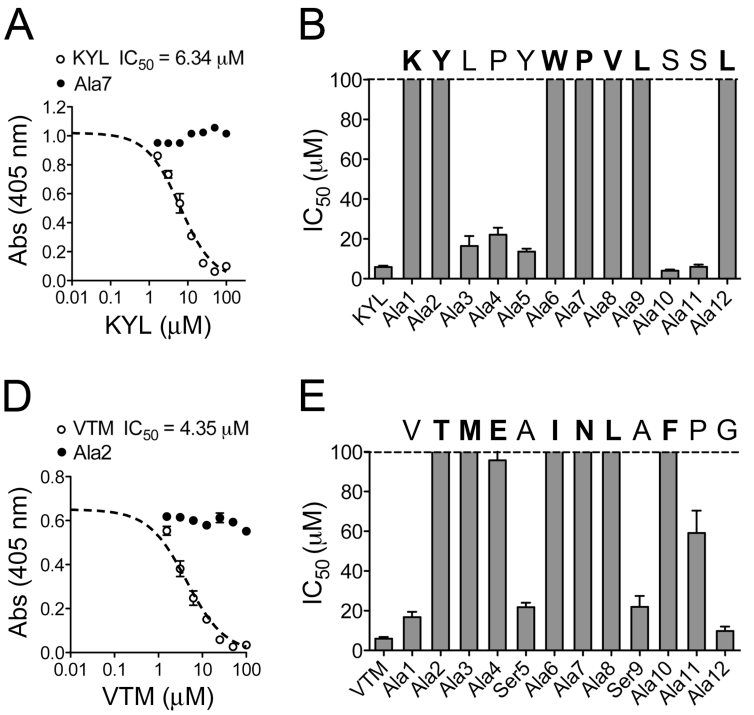

C

Peptide	Sequence	IC_{50} ± SE (μM)	n
KYL	KYLPYWPVLSSL	5.9 ± 0.66	12
Ala1	**A**YLPYWPVLSSL	>>100	3
Ala2	K**A**LPYWPVLSSL	>>100	3
Ala3	KY**A**PYWPVLSSL	16 ± 5.0	4
Ala4	KYL**A**YWPVLSSL	23 ± 3.5	3
Ala5	KYLP**A**WPVLSSL	14 ± 1.5	3
Ala6	KYLPY**A**PVLSSL	>>100	3
Ala7	KYLPYW**A**VLSSL	>>100	3
Ala8	KYLPYWP**A**LSSL	>>100	4
Ala9	KYLPYWPV**A**SSL	>100	3
Ala10	KYLPYWPVL**A**SL	3.5 ± 0.64	3
Ala11	KYLPYWPVLS**A**L	4.9 ± 1.2	3
Ala12	KYLPYWPVLSS**A**	>100	5

F

Peptide	Sequence	IC_{50} ± SE (μM)	n
VTM	VTMEAINLAFPG	5.9 ± 0.79	4
Ala1	**A**TMEAINLAFPG	16 ± 2.7	3
Ala2	V**A**MEAINLAFPG	>>100	3
Ala3	VT**A**EAINLAFPG	>>100	3
Ala4	VTM**A**AINLAFPG	95 ± 18.6	3
Ser5	VTME**S**INLAFPG	21 ± 2.2	3
Ala6	VTMEA**A**NLAFPG	>>100	3
Ala7	VTMEAI**A**LAFPG	>>100	3
Ala8	VTMEAIN**A**AFPG	>100	3
Ser9	VTMEAINL**S**FPG	22 ± 5.4	3
Ala10	VTMEAINLA**A**PG	>>100	3
Ala11	VTMEAINLAF**A**G	59 ± 11	3
Ala12	VTMEAINLAFP**A**	9.7 ± 2.2	3

Figure 4. Alanine scans of the KYL and VTM peptides identify peptide residues important for EphA4 binding

(**A**, **D**) Examples of curves for inhibition of the binding of EphA4 to ephrin-A5 by KYL, the inactive KYL-Ala7 (A), VTM, or the inactive VTM-Ala2 (D). (**B**,**E**) The histograms show average IC_{50} values ± SEM for the indicated modified forms of the KYL and VTM peptides. The IC_{50} values were calculated from inhibition curves similar to those shown in A and D. Ala1 to Ala12 are peptides where alanine replaces the indicated residue while Ser5 and Ser9 are peptides where serine replaces the original alanine at that position of VTM. The sequences of the peptides are shown above the histograms, with the residues identified as critical for binding to EphA4 in bold. (**C**,**F**) The tables show the average IC_{50} values ± SEM calculated from the indicated number of inhibition curves (n). >100 μM indicates that the average IC_{50} value was higher than 100 μM and too high to measure accurately; ≫100 μM indicates that no inhibition was detectable at 100 μM, which was the highest peptide concentration tested.

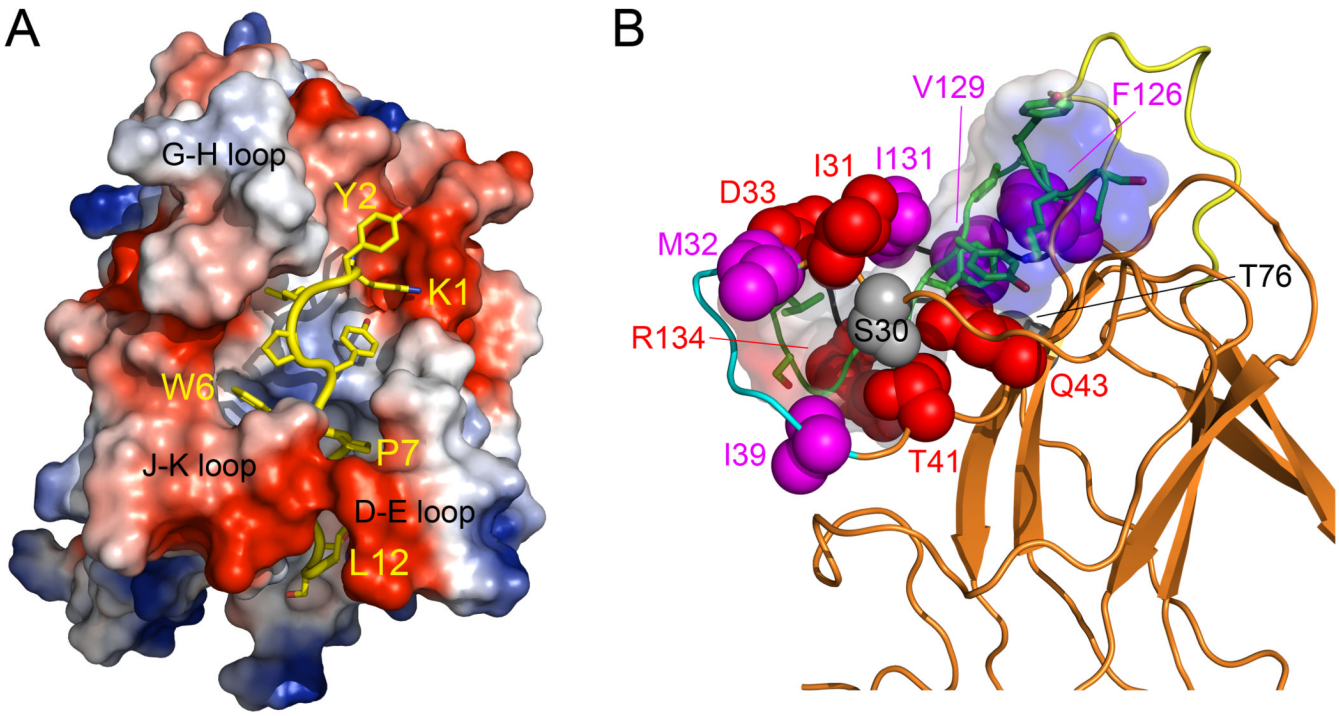

Figure 5. Docking model of the EphA4-KYL complex based on NMR chemical shift differences and the results of EphA4 mutagenesis and KYL alanine scanning

(**A**) Surface representation of the EphA4 ephrin-binding domain showing electrostatic potentials (blue: positive, red: negative, gray: neutral) and stick representation of the KYL peptide (yellow). KYL residues important for EphA4 binding are labeled, except for P7 and V8, which are hidden within the ephrin-binding pocket. (**B**) Ribbon representation of the EphA4 ephrin-binding domain (orange) and stick representation of the KYL peptide (green, with transparent electrostatic surface). Red and purple spheres represent EphA4 residues whose mutation to alanine results in loss or substantial reduction of KYL binding ability, respectively (Table 1). In addition, G132 is hidden behind D33 and A165 is hidden behind Q43. Gray spheres are used to depict EphA4 residues S30 and T76, which show direct contacts with the KYL peptide and are significantly perturbed in NMR spectra upon adding the KYL peptide, but whose mutation to alanine causes no detectable reduction in KYL binding ability. The EphA4 D–E loop is shown in cyan, the G–H loop in yellow, and the J–K loop in black.

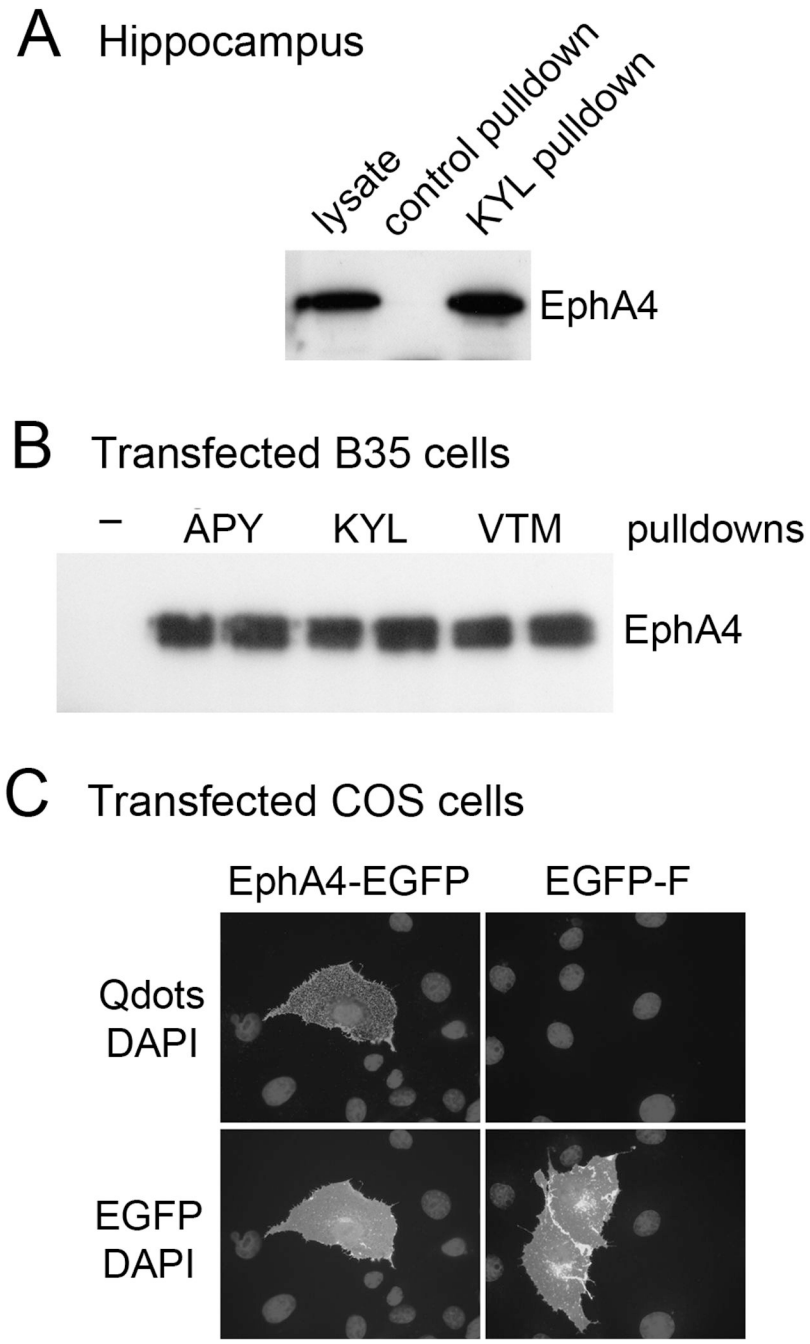

Figure 6. Use of KYL to purify EphA4 and image EphA4-expressing cells

(**A**) Biotinylated KYL peptide bound to streptavidin beads was used to pull down EphA4 from mouse hippocampal lysate. A biotinylated 12-mer peptide that does not bind EphA4 was used in a control pulldown. The proteins associated with the streptavidin beads and hippocampal lysate were probed by immunoblotting for EphA4. (**B**) Biotinylated APY, KYL and VTM peptides bound to streptavidin beads were used to pull down EphA4 from B35 neuroblastoma cells stably transfected with an EphA4 plasmid. Beads without a bound peptide were used in a control pulldowns (–). The proteins associated with the streptavidin beads were probed by immunoblotting for EphA4. Two lanes are shown for each peptide.

(**C**) COS cells were transiently transfected with the EphA4 extracellular and transmembrane regions fused to enhanced green fluorescent protein (EGFP) replacing the cyoplasmic region, or membrane-targeted farnesylated EGFP-F as a control, and labeled with KYL bound to red fluorescent quantum dots. The green fluorescent proteins and nuclei stained with DAPI were also imaged.

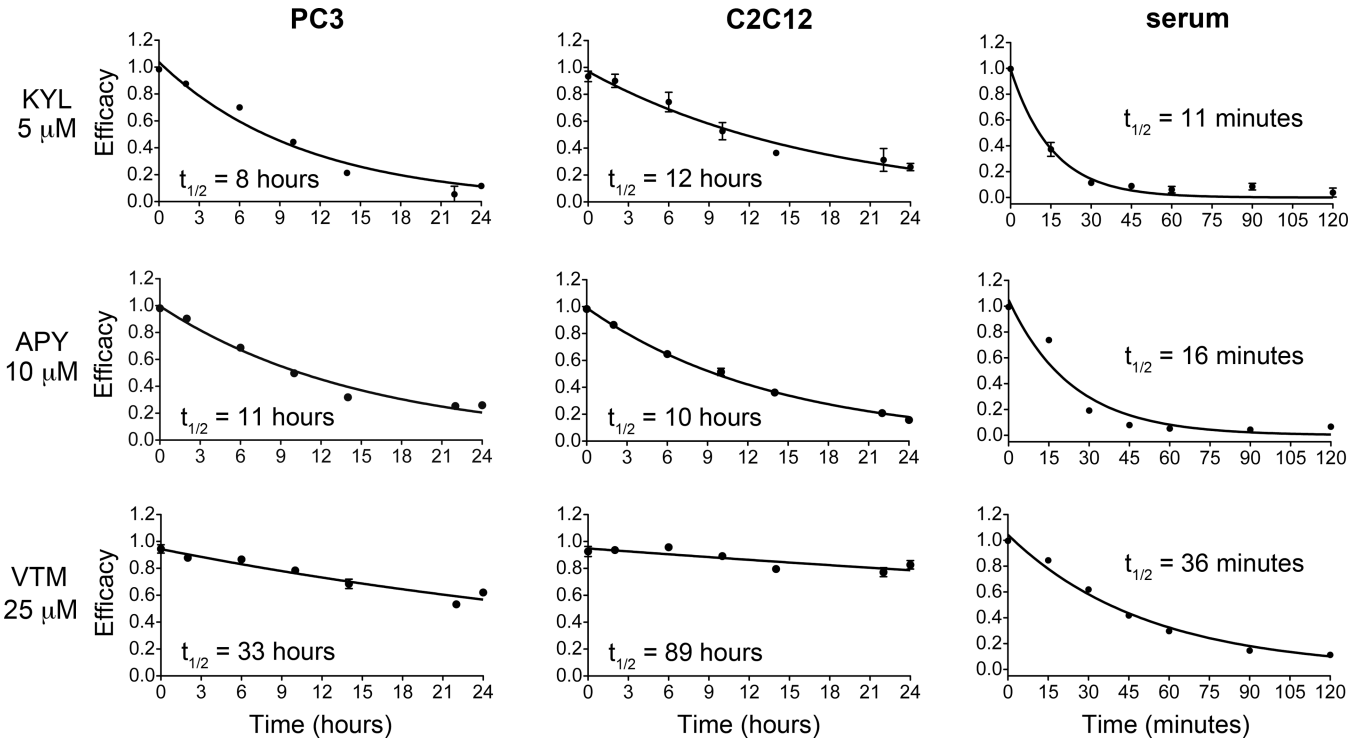

Figure 7. Stability of KYL, APY and VTM in cell conditioned medium or serum

The peptides were incubated in PC3 prostate cancer cell conditioned medium, C2C12 myoblast cell conditioned medium, or mouse serum for the indicated times at 37°C and then tested for inhibition of EphA4 AP binding to immobilized ephrin-A5 Fc. Efficacy represents the ability of the peptides to inhibit EphA4-ephrin-A5 interaction. The EphA4 AP signal obtained from wells incubated with conditioned medium or mouse serum not containing any peptide was used to determine the 0% inhibition level (efficacy = 0) and the signal obtained in the presence of intact peptides was used to determine maximal inhibition and for normalization (efficacy = 1). The peptide concentrations used inhibit EphA4 AP-ephrin-A5 Fc binding by ~80% in the absence of proteolytic degradation.

Table 1

Effects of EphA4 mutations on the interaction with ephrin-A5 and peptide ligands

EphA4 mutant[1]	residue in NP_004429	structural location[2]	ephrin-A5 binding	KYL binding	KYL inhibition	KYL CSD[3]	APY binding	APY inhibition	VTM binding	VTM inhibition
S30A	S58A	D β strand	=	=	=	>0.4	=	=	−	=
I31A	I59A	D β strand	=	− −	− −	>0.4	− −	− −	−	−
M32A	M60A	D β strand	−	−	+	>0.4	+	+	−	+
D33A	D61A	D–E loop	−	− −	+	>0.4	=	+	−	+
I39A	I67A	E β strand	=	−	−	<0.4	−	−	+	=
T41A	T69A	E β strand	=	− −	− −	>0.4	− −	− −	− −	− −
Q43A	Q71A	E β strand	−	− −	− −	>0.4	− −	− −	− −	− −
T76A	T104A	G β strand	− −	=	nd	>0.4	+	nd	++	nd
D123A	D151A	I–J loop	−	=	=	<0.4	−	−	+	=
F126A	F154A	I–J loop	− −	−	nd	<0.4	=	nd	−	nd
V129A	V157A	J β strand	=	−	−	<0.4	=	−	− −	− −
I131A	I159A	J–K loop	− −	−	nd	>0.4	=	nd	− −	nd
G132V	G160V	J–K loop	=	− −	− −	>0.4	=	− −	− −	− −
R134A	R162A	J–K loop	− −	− −	nd	nd	−	nd	− −	nd
M136A	M164A	K β strand	−	=?	+	nd	+	+	− −	− −
A165S	A193S	M β strand	−	− −	− −	>0.4	− −	− −	− −	=

[1] Numbering is according to the construct used, where N29 in GenBank accession number NP_004429 is the first residue [45].

[2] According to ref. [35].

[3] CSD, chemical shift difference. − −, very low or absent binding/inhibition; −, substantially less than wild-type; =, similar to wild-type; +, more than wild-type; ++, much more than wild-type; ? indicates high variability in multiple experiments. nd, not determined. Residues that have not been reported to interact with ephrin ligands in EphA4 or other Eph receptors [35] are underlined.